Detection of Scalar Couplings Across NH···OP and OH···OP Hydrogen Bonds in a Flavoprotein

Frank Löhr,[†] Stephen G. Mayhew,[‡] and Heinz Rüterjans*,[†]

Contribution from the Institut für Biophysikalische Chemie, Johann Wolfgang Goethe-Universität, Biozentrum N230, Marie Curie-Strasse 9, 60439 Frankfurt am Main, Germany, and Department of Biochemistry, University College Dublin, Belfield, Dublin 4, Ireland

Received April 17, 2000. Revised Manuscript Received June 28, 2000

Abstract: Hydrogen bonding plays a major role in the tight binding of the FMN cofactor in flavodoxins. The present NMR investigation provides direct experimental evidence for hydrogen bonds involving the phosphate moiety of FMN in *Desulfovibrio vulgaris* flavodoxin. Several trans-hydrogen bond *J* couplings between the phosphorus nucleus and backbone amide as well as side chain hydroxyl protons of the apoprotein have been detected. It is shown that relaxation interference between ^{1}H chemical shift anisotropy and ^{1}H−^{31}P dipolar interactions can also lead to correlations of these nuclei in HMBC spectra. The size of the $^{2h}J_{PH}$ coupling constants was determined using a simple ^{31}P-detected quantitative *J* correlation experiment. For at least one amide group a scalar three-bond coupling between the phosphorus and nitrogen has been observed in a [^{15}N,^{1}H]-TROSY-type ^{15}N−{^{31}P} spin−echo difference experiment. With approximately 1.7 Hz its magnitude is larger than that of the ^{31}P−^{1}H couplings, which ranged from 0.5 to 1.6 Hz.

Introduction

Flavodoxins are small acidic flavoproteins that utilize riboflavin 5′-monophosphate (FMN) as the only redox active component in a variety of biological electron-transfer reactions.[1] Their structures in all three accessible oxidation states are well-characterized by both X-ray crystallographic[2] and NMR[3] studies and proved to be virtually identical in the crystal and in solution. Although differences in the immediate vicinity of the prosthetic group, responsible for a modulation of its redox potentials, were observed among flavodoxins from different species, it is undisputed that hydrogen bonding plays an important role for its strong binding to the apoprotein. Important criteria for NMR detection of hydrogen bonds are, among others, protection of exchange of labile protons with solvent,[4] ^{2}H/^{1}H fractionation factors,[5] isotropic ^{1}H chemical shifts,[5c,6] and chemical shift anisotropy (CSA).[6b,7] As recently demonstrated, more direct evidence is available by detection of scalar couplings across hydrogen bonds (^{h}J), allowing an identification of both donor and acceptor groups. Examples for such couplings include (i) $^{2h}J(^{113}\mathrm{Cd}-^{1}\mathrm{H})$[8] and $^{2h}J(^{199}\mathrm{Hg}-^{1}\mathrm{H})$[8b] in a metalloprotein, (ii) $^{3h}J(^{1}\mathrm{H}-^{1}\mathrm{H})$ in galactose-derived pyranoses,[9] (iii) $^{2h}J(^{15}\mathrm{N}-^{15}\mathrm{N})$,[10,11] $^{1h}J(^{15}\mathrm{N}-^{1}\mathrm{H})$,[11] $^{4h}J(^{15}\mathrm{N}-^{15}\mathrm{N})$,[12] and $^{3h}J(^{15}\mathrm{N}-^{13}\mathrm{CO})$[13] in nucleic acid base pairs, (iv) $^{1h}J(^{19}\mathrm{F}-^{1}\mathrm{H})$ and $^{2h}J(^{19}\mathrm{F}-^{19}\mathrm{F})$ in clusters of the fluoride ion with HF,[14] (v) $^{1h}J(^{15}\mathrm{N}-^{1}\mathrm{H})$ and $^{2h}J(^{15}\mathrm{N}-^{19}\mathrm{F})$ in a complex between HF and a pyridine derivative,[15] (vi) side chain−side chain $^{2h}J(^{15}\mathrm{N}-^{15}\mathrm{N})$ between two histidine residues in apomyoglobin,[16] and (vii) $^{3h}J(^{15}\mathrm{N}-^{13}\mathrm{C}')$,[17] $^{2h}J(^{1}\mathrm{H}^{\mathrm{N}}-^{13}\mathrm{C}')$,[18] and $^{3h}J(^{1}\mathrm{H}^{\mathrm{N}}-^{13}\mathrm{C}^{\alpha})$[19] in the backbone of various proteins. In the present study we focus on hydrogen bond

† Institut für Biophysikalische Chemie, University Frankfurt.
‡ Department of Biochemistry, University College Dublin.
* Address correspondence to this author: Institut für Biophysikalische Chemie.

(1) (a) Mayhew, S. G.; Ludwig, M. L. In *The Enzymes*; Boyer, P. D., Ed.; Academic Press: New York, 1975; Vol. 12, pp 57−118. (b) Mayhew, S. G.; Tollin, G. In *Chemistry and Biochemistry of Flavoenzymes*; Müller, F., Ed.; CRC Press: Boca Raton, 1992; Vol. III, pp 389−426. (c) Ludwig, M. L.; Luschinsky, C. L. In *Chemistry and Biochemistry of Flavoenzymes*; Müller, F., Ed.; CRC Press: Boca Raton, 1992; Vol. III, pp 427−466. (d) Vervoort, J.; Heering, D.; Peelen, S.; van Berkel, W. *Methods Enzymol.* **1994**, *243*, 188−203.

(2) (a) Watenpaugh, K. D.; Sieker, L. C.; Jensen, L. H.; Dubourdieu, M. *Proc. Natl. Acad. Sci. U.S.A.* **1972**, *69*, 3185−3188. (b) Andersen, R. D.; Apgar, P. A.; Burnett, R. M.; Darling, G. D.; LeQuesne, M. E.; Mayhew, S. G.; Ludwig, M. L. *Proc. Natl. Acad. Sci. U.S.A.* **1972**, *69*, 3189−3191. (c) Smith, W. W.; Burnett, R. M.; Darling, G. D.; Ludwig, M. L. *J. Mol. Biol.* **1977**, *117*, 195−225. (d) Smith, W. W.; Pattridge, K. A.; Ludwig, M. L.; Petsko, G. A.; Tsernoglou, D.; Tanaka, M.; Yasunobu *J. Mol. Biol.* **1983**, *165*, 737−755. (e) Fukuyama, K.; Wakabayashi, S.; Matsubara, H.; Rogers, L. J. *J. Biol. Chem.* **1990**, *265*, 15804−15812. (f) Watt, W.; Tulinsky, A.; Swenson, R. P.; Watenpaugh, K. D. *J. Mol. Biol.* **1991**, *218*, 195−208. (g) Rao, S. T.; Shaffie, F.; Yu, C.; Satyshur, K. A.; Stockman, B. J.; Markley, J. L.; Sundaralingam, M. *Protein Sci.* **1992**, *1*, 1413−1427. (h) Fukuyama, K.; Matsubara, H.; Rogers, L. J. *J. Mol. Biol.* **1992**, *225*, 775−789. (i) Walsh, M. A. Ph.D. Thesis, National University of Ireland, 1994. (j) Burkhart, B. M.; Ramakrishnan, B.; Yan, H.; Reedstrom, R. J.; Markley, J. L. Straus, N. A.; Sundaralingham, M. *Acta Crystallogr.* **1995**, *D51*, 318−330. (k) Sharkey, C. T.; Mayhew, S. G.; Higgins, T. M.; Walsh, M. A. In *Flavins and Flavoproteins*; Stevenson, K. J., Massey, V., Williams, C. H., Jr., Eds.; University of Calgary Press: Calgary, 1996; pp 445−448. (l) Romero, A.; Caldeira, J.; LeGall, J.; Moura, I.; Moura, J. J. G.; Romao, M. J. *Eur. J. Biochem.* **1996**, *239*, 190−196. (m) Hoover, D. M.; Ludwig, M. L. *Protein Sci.* **1997**, *6*, 2525−2537. (n) Walsh, M. A.; McCarthy, A.; O'Farrell, P. A.; McArdle, P.; Cunningham, P. D.; Mayhew, S. G.; Higgins, T. M. *Eur. J. Biochem.* **1998**, *258*, 362−371. (o) Drennan, C. L.; Pattridge, K. A.; Weber, C. H.; Metzger, A. L.; Hoover, D. M.; Ludwig, M. L. *J. Mol. Biol.* **1999**, *294*, 711−724.

(3) (a) van Mierlo, C. P. M.; Lijnzaad, P.; Vervoort, J.; Müller, F.; Berendsen, H. J. C.; de Vlieg, J. *Eur. J. Biochem.* **1990**, *194*, 185−198. (b) Stockman, B. J.; Krezel, A. M.; Markley, J. L.; Leonhardt, K. G.; Straus, N. A. *Biochemistry* **1990**, *29*, 9600−9609. (c) Clubb, R. T.; Thanabal, V.; Osborne, C.; Wagner, G *Biochemistry* **1991**, *30*, 7718−7730. (d) Stockman, B. J.; Richardson, T. E.; Swenson, R. P. *Biochemistry* **1994**, *33*, 15298−15308. (e) Knauf, M.; Löhr, F.; Blümel, M.; Mayhew, S. G.; Rüterjans, H. *Eur. J. Biochem.* **1996**, *238*, 423−434. (f) Peelen, S.; Wijmenga, S. S.; Erbel, P. J. A.; Robson, R. L.; Eady, R. R.; Vervoort, J. *J. Biomol. NMR* **1996**, *7*, 315−330. (g) Ponstingl, H.; Otting, G. *Eur. J. Biochem.* **1997**, *244*, 384−399. (h) Steensma, E.; Nijman, M. J. M.; Bollen, Y. J. M.; de Jager, P. A.; van den Berg, W. A. M.; van Dongen, W. M. A. M.; van Mierlo, C. P. M. *Protein Sci.* **1998**, *7*, 306−317.

(4) (a) Hvidt, A.; Nielsen, S. O. *Adv. Protein Chem.* **1966**, *21*, 287−386. (b) Wagner, G. *Q. Rev. Biophys.* **1983**, *16*, 1−57. (c) Englander, S. W.; Kallenbach, N. R. *Q. Rev. Biophys.* **1983**, *16*, 521−655.

10.1021/ja001345k CCC: $19.00
Published on Web 09/08/2000

interactions in flavodoxin from the sulfate-reducing bacteria *Desulfovibrio vulgaris* (strain Hildenborough), involving the phosphate of FMN in the oxidized (quinone) state.

The molecule investigated here contains a single polypeptide chain of 147 amino acid residues, forming a central, five-stranded parallel β-sheet and two α-helices on each side. The cofactor is mostly bound below the protein surface and makes contacts with three loop regions, i.e., residues 10−15, 58−62, and 95−102. From ^{31}P NMR studies it is known that the FMN 5′-phosphate group is dianionic when bound to apoflavodoxin, independent of the redox state.[20] The absence of basic residues in the phosphate binding site which is highly conserved among all flavodoxins precludes any favorable electrostatic interactions. Instead, the negative charge is stabilized by extensive hydrogen bonding with the backbone and side chains of the apoprotein as illustrated in Figure 1 for the *D. vulgaris* species. Hydrogen bonds are formed with amide and/or hydroxyl groups of residues Ser10, Thr11, Thr12, Asn14, Thr15, and Ser58, as implied by short distances observed in its crystal structures.[2a,f,i,n] NMR assignments have been obtained for its backbone ^{1}H and ^{15}N nuclei[22] as well as for side chain hydroxyl protons[22a,23] by use of ^{1}H−^{15}N and ^{1}H−^{1}H correlation experiments. Characteristic low-field amide ^{1}H and, in the case of Thr11 and Thr15, ^{15}N chemical shifts and unusually slow exchange with the solvent of Ser10, Thr12, Thr15, and Ser58 hydroxyl protons, which is a prerequisite for their NMR detection, suggests that a very similar hydrogen bond network exists in solution. In an attempt to directly probe these hydrogen bonds we have carried out NMR experiments that rely on scalar couplings involving the phosphate ^{31}P nucleus.

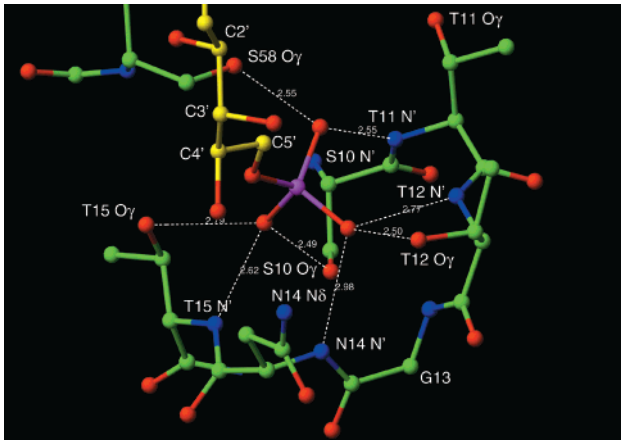

Figure 1. Ball-and-stick model of the phosphate binding site in *Desulfovibrio vulgaris* flavodoxin. Shown is the ribityl-phosphate moiety of FMN and the amino acid residues of apoflavodoxin potentially involved in hydrogen bond interactions with the phosphate. Carbon atoms of the apoprotein and the ribityl chain are drawn in green and yellow, respectively. Backbone N···OP and side chain O···OP distances <3 Å are indicated. The figure was prepared with MOLMOL[21] using the X-ray coordinates of ref 2i.

Results and Discussion

Detection of $^{h}J_{HP}$ Couplings. The most sensitive NMR pulse sequence for correlating ^{31}P with ^{1}H is the HMBC.[24] Since *D. vulgaris* flavodoxin gives rise to a single phosphorus resonance the experiment could be performed without evolution of its chemical shift, providing simple one-dimensional ^{31}P-edited ^{1}H spectra. Gradient coherence selection was employed to effectively suppress proton resonances not coupled to phosphorus. The corresponding spectrum of a 7 mM flavodoxin sample, recorded at 800 MHz proton frequency, is shown in Figure 2A. The spectrum exhibits intense signals at the resonance positions of Thr12 OH, Thr15 NH, and Thr15 OH as well as a weak signal for Thr11 NH. Very weak correlations due to other putatively hydrogen bonded protons cannot be excluded, but the signal-to-noise ratio is too low to allow their unambiguous

(5) (a) Loh, S. N.; Markley, J. L. *Biochemistry* **1994**, *33*, 1029−1036. (b) Bowers, P. M.; Klevit, R. E. *Nat., Struct. Biol.* **1996**, *3*, 522−531. (c) Harris, T. K.; Mildvan, A. S. *Proteins: Struct., Funct., Genet.* **1999**, *35*, 275−282. (d) Bowers, P. M.; Klevit, R. E. *J. Am. Chem. Soc.* **2000**, *122*, 1030−1033.

(6) (a) Shoup, R. R.; Miles, H. T.; Becker, E. D. *Biochem. Biophys. Res. Commun.* **1966**, *23*, 194−201. (b) Berglund, B.; Vaughan, R. W. *J. Chem. Phys.* **1980**, *73*, 2037−2043. (c) Wagner, G.; Pardi, A.; Wüthrich, K. *J. Am. Chem. Soc.* **1983**, *105*, 5948−5949. (d) de Dios, A. C.; Pearson, J. G.; Oldfield, E. *Science* **1993**, *260*, 1491−1496.

(7) (a) Tjandra, N.; Bax, A. *J. Am. Chem. Soc.* **1997**, *119*, 8076−8082. (b) Tessari, M.; Vis, H.; Boelens, R.; Kaptein, R.; Vuister, G. W. *J. Am. Chem. Soc.* **1997**, *119*, 8985−8990.

(8) (a) Blake, P. R.; Park, J. B.; Adams, M. W. W.; Summers, M. F. *J. Am. Chem. Soc.* **1992**, *114*, 4931−4933. (b) Blake, P. R.; Lee, B.; Summers, M. F.; Adams, M. W. W.; Park, J. B.; Zhou, Z. H.; Bax, A. *J. Biomol. NMR* **1992**, *2*, 527−533.

(9) Kwon, O.; Danishefsky, S. J. *J. Am. Chem. Soc.* **1998**, *120*, 1588−1599.

(10) (a) Dingley, A. J.; Grzesiek, S. *J. Am. Chem. Soc.* **1998**, *120*, 8293−8297. (b) Wöhnert, J.; Dingley, A. J.; Stoldt, M.; Görlach, M.; Grzesiek, S.; Brown, L. R. *Nucleic Acids Res.* **1999**, *27*, 3104−3110. (c) Majumdar, A.; Kettani, A.; Skripkin, E. *J. Biomol. NMR* **1999**, *14*, 67−70. (d) Majumdar, A.; Kettani, A.; Skripkin, E.; Patel, D. J. *J. Biomol. NMR* **1999**, *15*, 207−211. (e) Hennig, M.; Williamson, J. R. *Nucleic Acids Res.* **2000**, *28*, 1585−1593.

(11) (a) Pervushin, K.; Ono, A.; Fernández, C.; Szyperski, T.; Kainosho, M.; Wüthrich, K. *Proc. Natl. Acad. Sci. U.S.A.* **1998**, *95*, 14147−14151. (b) Dingley, A. J.; Masse, J. E.; Peterson, R. D.; Barfield, M.; Feigon, J.; Grzesiek, S. *J. Am. Chem. Soc.* **1999**, *121*, 6019−6027. (c) Pervushin, K.; Fernández, C.; Riek, R.; Ono, A.; Kainosho, M.; Wüthrich, K. *J. Biomol. NMR* **2000**, *16*, 39−46.

(12) Liu, A.; Majumdar, A.; Hu, W.; Kettani, A.; Skripkin, E.; Patel, D. J. *J. Am. Chem. Soc.* **2000**, *122*, 3206−3210.

(13) Dingley, A. J.; Masse, J. E.; Feigon, J.; Grzesiek, S. *J. Biomol. NMR* **2000**, *16*, 279−289.

(14) Shenderovich, I. G.; Smirnov, S. N.; Denisov, G. S.; Gindin, V. A.; Golubev, N. S.; Dunger, A.; Reibke, R.; Kirpekar, S.; Malkina, O. L.; Limbach, H. H. *Ber. Bunsen-Ges. Phys. Chem.* **1998**, *102*, 422−428.

(15) Golubev, N. S.; Shenderovich, I. G.; Smirnov, S. N.; Denisov, G. S.; Limbach, H. H. *Chem. Eur. J.* **1999**, *5*, 492−497.

(16) Hennig, M.; Geierstanger, B. H. *J. Am. Chem. Soc.* **1999**, *121*, 5123−5126.

(17) (a) Cordier, F.; Grzesiek, S. *J. Am. Chem. Soc.* **1999**, *121*, 1601−1602. (b) Cornilescu, G.; Hu, J.-S.; Bax, A. *J. Am. Chem. Soc.* **1999**, *121*, 2949−2950. (c) Wang, Y.-X.; Jacob, J.; Cordier, F.; Wingfield, P.; Stahl, S. J.; Lee-Huang, S.; Torchia, D.; Grzesiek, S.; Bax, A. *J. Biomol. NMR* **1999**, *14*, 181−184.

(18) (a) Cordier, F.; Rogowski, M.; Grzesiek, S.; Bax, A. *J. Magn. Reson.* **1999**, *140*, 510−512. (b) Meissner, A.; Sørensen, O. W. *J. Magn. Reson.* **2000**, *143*, 387−390.

(19) Meissner, A.; Sørensen, O. W. *J. Magn. Reson.* **2000**, *143*, 431−434.

(20) (a) Edmondson, D. E.; James, T. L. *Proc. Natl. Acad. Sci. U.S.A.* **1979**, *76*, 3786−3789. (b) Favaudon, V.; LeGall, J.; Lhoste, J. M. In *Flavins and Flavoproteins*; Yagi, K., Yamano, T., Eds.; Japan Scientific Societies Press: Tokyo, 1980; pp 373−386. (c) Moonen, C. T. W.; Müller, F. *Biochemistry* **1982**, *21*, 408−414. (d) Vervoort, J.; Müller, F.; Mayhew, S. G.; van den Berg, W. A. M.; Moonen, C. T. W.; Bacher, A. *Biochemistry* **1986**, *25*, 6789−6799. (e) Vervoort, J.; van Berkel, W. J. H.; Mayhew, S. G.; Müller, F.; Bacher, A.; Nielsen, P.; LeGall, J. *Eur. J. Biochem.* **1986**, *161*, 749−756. (f) Stockman, B. J.; Westler, W. M.; Mooberry, E. S.; Markley, J. L. *Biochemistry* **1988**, *27*, 136−142. (g) Thorneley, R. N. F.; Abell, C.; Ashby, G. A.; Drummond, M. H.; Eady, R. R.; Huff, S.; MacDonald, C. J.; Shneier, A. *Biochemistry* **1992**, *31*, 1216−1224.

(21) Koradi, R.; Billeter, M.; Wüthrich, K. *J. Mol. Graph.* **1996**, *14*, 51−55.

(22) (a) Knauf, M. A.; Löhr, F.; Curley, G. P.; O'Farrell, P.; Mayhew, S. G.; Müller, F.; Rüterjans, H. *Eur. J. Biochem.* **1993**, *213*, 167−184. (b) Stockman, B. J.; Euvrard, A.; Kloosterman, D. A.; Scahill, T. A.; Swenson, R. P. *J. Biomol. NMR* **1993**, *3*, 133−149.

(23) Peelen, S.; Vervoort, J. *Arch. Biochem. Biophys.* **1994**, *314*, 291−300.

(24) Bax, A.; Summers, M. F. *J. Am. Chem. Soc.* **1986**, *108*, 2093−2094.

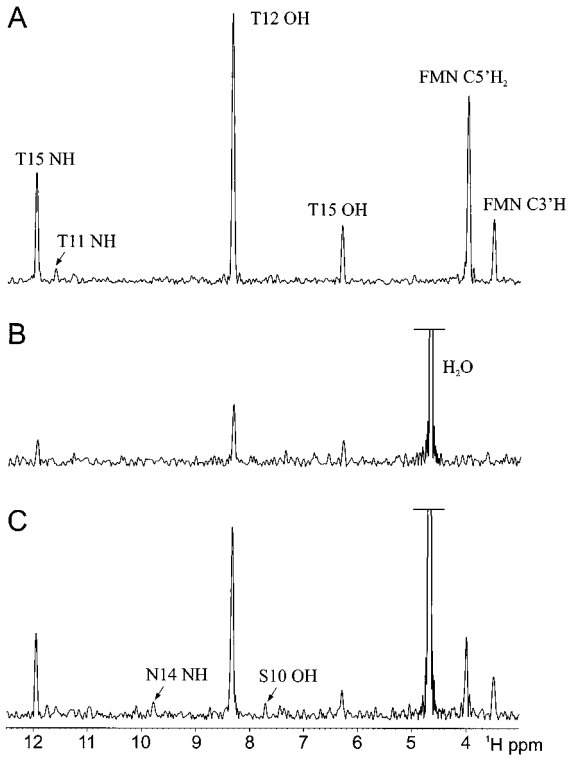

Figure 2. 1D [^{1}H,^{31}P]-HMBC spectra of oxidized *D. vulgaris* flavodoxin recorded with Δ delays of 20 ms. Signals in spectra A, B, and C arise from both ^{1}H−^{31}P scalar and cross correlation interactions, exclusively from ^{1}H CSA/^{1}H−^{31}P dipolar cross correlation, and exclusively from scalar couplings, respectively. The ^{1}H acquisition time was 46 ms. After multiplication with a 22.5° shifted sine-bell function, FID's were transformed in the absolute value mode. Vertical scales for spectra B and C are identical while that of spectrum A is compressed by a factor of 2. Note that the same number of scans were used to record B and C, but a larger number were used to record spectrum A. Proton resonance assignments are indicated. The incomplete suppression of the water signal in B and C is a consequence of the additional ^{1}H 180° pulse in the applied pulse sequences.

identification. The signal at 4.0 and presumably also the one at 3.5 ppm arise from regular through-bond *J* connectivities with FMN ribityl chain protons. Their chemical shifts were independently assigned in an HCCH-COSY spectrum of ^{13}C-labeled flavodoxin (F. Löhr, unpublished results). The degenerate C5′ methylene protons are coupled to the phosphorus via $^3J_{PH}$ while the tentatively assigned C3′H−P correlation would correspond to an unusual five-bond coupling. Such $^5J_{PH}$ couplings are not normally observed, e.g. in nucleic acids, however, ^{1}H−^{113}Cd and ^{1}H−^{199}Hg five-bond *J* couplings have been reported for a rubredoxin.[8b] Partial overlap with the C5′H$_2$ signal hampers the identification of a possible $^4J_{PH}$ interaction of C4′H (δ 3.90 ppm). It should be mentioned that similar experiments have been carried out on *Azotobacter* flavodoxin[25] but no ^{1}H−^{31}P correlations involving the FMN phosphorus were detected which may be attributed to a lower sensitivity at the magnetic field strength (360 MHz) employed.

Two aspects of the through-hydrogen bond correlations revealed by the spectrum of Figure 2A deserve further investigation. First, although the signal intensities in HMBC spectra provide a rough estimate of the relative size of the underlying interactions, a more quantitative evaluation is impossible due to the antiphase fine structure. Second, it is unclear whether scalar coupling is the sole mechanism for the polarization transfer. While it is unlikely that residual dipolar couplings[26] contribute significantly (see below), it cannot be excluded a priori that relaxation interference between ^{1}H chemical shift anisotropy and ^{1}H−^{31}P dipolar (DD) interactions[7,27] is responsible for the observed effects. Using (O)H···P and (N)H···P distances derived from the X-ray structure of flavodoxin[2i] and CSA values of hydroxyl[6b] and amide[7] protons taken from the literature the buildup of ^{1}H−^{31}P antiphase magnetization through ^{1}H CSA/^{1}H−^{31}P DD relaxation interference during the Δ period of the HMBC experiment can be estimated. Depending on the relative orientation of the CSA tensor and the internuclear vector the cross correlated relaxation can mimic J_{HP} couplings of up to approximately 0.6 and 0.4 Hz for OH and NH hydrogens, respectively, where upper limits of ^{1}H chemical shift anisotropy ($\sigma_{\parallel}-\sigma_{\perp}$) of 20 and 30 ppm and a correlation time τ_c of 6 ns were assumed. These values may well be in the order of scalar interactions through hydrogen bonds.

To investigate the latter issue experimentally, the [^{1}H,^{31}P]-HMBC was repeated with a slight modification of the pulse sequence, consisting of an additional ^{1}H 180° pulse centered in the delay Δ for the buildup of ^{1}H antiphase magnetization with respect to ^{31}P. This pulse refocuses scalar couplings whereas CSA/DD cross correlation remains active and allows ^{1}H,^{31}P multiple quantum coherence, selected by pulsed field gradients, to be created by the following ^{31}P 90° pulse. Application of the pulse sequence to flavodoxin yielded the spectrum depicted in Figure 2B. Three signals, corresponding to the hydrogen-bonded hydroxyls of Thr12 and Thr15 and the amide of Thr15, are readily apparent, indicating that their interaction with the FMN phosphorus via the CSA/DD cross-correlation mechanism is not negligible, in accordance with the theoretical calculation. In contrast, no polarization transfer occurred for the FMN ribityl protons that are covalently attached to the phosphorus via three and five bonds, respectively, presumably because of a comparatively small anisotropy of their chemical shift tensors and the larger distances. To assess the relative contributions of scalar couplings and cross correlation a complementary [^{1}H,^{31}P]-HMBC experiment, in which a polarization transfer through *J* couplings takes place exclusively, was performed as well. This was achieved by simultaneously applying 180° pulses on protons and phosphorus in the middle of the Δ period, thus suppressing CSA/DD cross correlation.[7,28] The spectrum (Figure 2C) resulting from this version of the HMBC pulse sequence demonstrates that scalar coupling is the dominating effect in the case of Thr15 NH and Thr12 OH, while scalar coupling and cross correlation contribute approximately equally for Thr15 OH. Remarkably, additional signals of low intensity are observed at 9.78 and 7.72 ppm. These resonances were assigned to Asn14 amide and Ser10 hydroxyl protons,[22a] respectively, which are supposed to be hydrogen bonded to the phosphate group as well. The reason they could be detected in the spectrum of Figure 2C and, despite a longer accumulation time, not in the one of Figure 2A is still unclear. A possible explanation could be a dephasing of magnetization due to chemical exchange, the effect of which is reduced by the ^{1}H refocusing pulse applied during Δ when recording the spectrum of Figure 2C. It should be mentioned that CSA/DD relaxation interference in addition gives rise to dynamic frequency shifts which can, in principle, also lead to

(25) Live, D. H.; Edmondson, D. E. *J. Am. Chem. Soc.* **1988**, *110*, 4468−4470.

(26) (a) Tolman, J. R.; Flanagan, J. M.; Kennedy, M. A.; Prestegard, J. M. *Proc. Natl. Acad. Sci. U.S.A.* **1995**, *92*, 9279−9283. (b) Tjandra, N.; Grzesiek, S.; Bax, A. *J. Am. Chem. Soc.* **1996**, *118*, 6264−6272.

(27) (a) Goldman, M. *J. Magn. Reson.* **1984**, *60*, 437−452. (b) Tjandra, N.; Szabo, A.; Bax, A. *J. Am. Chem. Soc.* **1996**, *118*, 6986−6991.

(28) Palmer, A. G., III; Skelton, N. J.; Chazin, W. J.; Wright, P. E.; Rance, M. *Mol. Phys.* **1992**, *75*, 699−711.

apparent *J* correlations.[26b,29] While this effect is not eliminated in the pulse sequences employed here, its size is too small to contribute significantly to the observed couplings.

Quantitative Determination of ^{1}H−^{31}P Coupling Constants. As mentioned above, even a qualitative assessment of the magnitude of the detected ^{1}H−^{31}P scalar couplings is impeded primarily because of the antiphase character of signals in HMBC spectra. At the expense of a loss in sensitivity this problem might be circumvented by refocusing the active coupling before acquisition in an HMQC manner,[30] but the translation of signal amplitudes into coupling constants also requires calibration of the relevant ^{1}H signal amplitudes without selection of the magnetization transferred to the phosphorus. Due to signal overlap this cannot generally be achieved in 1D proton spectra of molecules of the size of flavodoxin. As far as amide protons are concerned, 2D ^{1}H−^{15}N correlated reference spectra may be recorded using isotopically labeled protein, but in the case of hydroxyl protons only homonuclear correlation spectroscopy would be feasible. A suitable pulse sequence has been introduced for the measurement of $^3J(^1\mathrm{H3'}-^{31}\mathrm{P})$ in nucleic acids.[31] However, this experiment was not attempted here for the following reasons: (i) it would rely on relatively small $^3J_{HH}$ couplings to detect even smaller $^3J_{HP}$ couplings, resulting in a low sensitivity; (ii) the OH−H$^\beta$ region of 2D ^{1}H−^{1}H correlation spectra is not sufficiently resolved for all relevant serine and threonine residues of flavodoxin; and (iii) the lack of an appropriate solvent suppression scheme might lead to an intense residual water signal for a protein sample dissolved in H_2O, making it difficult to quantitatively evaluate signal intensities at the serine and threonine H$^\beta$-resonance positions. As an alternative, a simple quantitative *J* correlation[32] experiment was employed in which scalar coupling de- and rephasing takes effect on transverse ^{31}P magnetization. The pulse scheme is loosely related to the LRCH experiment[33] and represents a 2D ^{31}P-detected [^{31}P,^{1}H]-HMQC with chemical shift evolution of scalar coupled protons in the indirect dimension. Advantages over the reverse polarization transfer pathway are, first, that no dephasing of ^{31}P magnetization due to homonuclear couplings occurs and, second, that the reference intensity required to calculate the desired heteronuclear coupling constants is measured in a ^{31}P rather than in a ^{1}H spectrum, thus avoiding overlap problems. On the other hand, ^{31}P detection is considerably less sensitive compared to proton detection. To reduce the contribution of CSA to phosphorus transverse relaxation, experiments were performed at lower field (500 MHz proton frequency).

The actual pulse sequence used is given in the Experimental Section. In quantitative *J* correlation, reference signal intensities are usually recorded in a separate experiment, which would yield a single phosphorus signal in the present case. Following a previously described procedure,[34] we have employed a modified phase cycle which provides cross-peaks together with the reference peak in a single spectrum. The latter appears as an axial peak at the carrier position in the indirect ^{1}H dimension. The utility of the pulse sequence was initially tested with de- and rephasing delays Δ ranging from 25 to 40 ms, the highest sensitivity being obtained for values around 30 ms. Figure 3A shows the result of a measurement with Δ = 30 ms. The 1D section along F1 is taken at the position of the FMN phosphorus resonance. It contains an intense axial signal, which corresponds to the fraction of ^{31}P magnetization not transferred to protons, as well as several cross-peaks at the chemical shifts of protons interacting with the phosphorus nucleus. With the exception of the Asn14 amide, signals are visible for all protons that were already detected in the HMBC spectra of Figure 2 and, in addition, for Thr12 NH and Ser58 OH, also presumed to be involved in the hydrogen bond network of the FMN 5′-phosphate group. The low signal-to-noise of the maxima at the positions of Thr11 NH, Thr12 NH, Ser58 OH, and Ser10 OH may call the existence of significant scalar interactions into question: however, they were present in all spectra acquired with this pulse sequence. It is interesting to note that a $^{2h}J_{PH}$ coupling with the Ser58 hydroxyl proton could be measured here but was not detectable in any of the [^{1}H,^{31}P]-HMBC experiments shown in Figure 2 despite their higher sensitivity. Presumably the reason is that the ^{31}P-detected method is considerably less prone to hydrogen exchange with the solvent which may be more significant for the Ser58 OH than for the other hydroxyls.

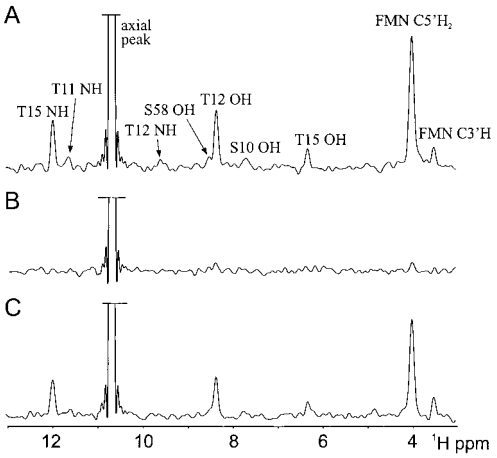

Figure 3. Traces along F1 from quantitative 2D ^{31}P−^{1}H correlation spectra taken at the ^{31}P chemical shift of the FMN phosphate resonance of flavodoxin (4.96 ppm). In parts B and C, respectively, only ^{31}P CSA/^{31}P−^{1}H dipolar cross correlation or only J_{PH} couplings would give rise to observable cross-peaks, whereas in part A both interactions can in principle contribute. Durations of the Δ periods were set to 30 ms for the spectrum in part A and to 32 ms for the spectra in parts B and C. The vertical scaling is the same in all spectra. The intense (truncated) signal labeled "axial peak" has been used as reference intensity to calculate coupling constants.

Again, relaxation interference, in this case between ^{31}P CSA and ^{31}P−^{1}H DD interactions, might be the cause of the polarization transfer. This effect was experimentally separated from scalar couplings in an analogous manner as described above for the 1D [^{1}H,^{31}P]-HMBC method. The spectrum of Figure 3B, in which the contribution of cross correlated relaxation is selected while scalar couplings are suppressed, is virtually free of cross-peaks, indicating that this effect is negligible in the ^{31}P detected [^{31}P,^{1}H]-HMQC, presumably because of a considerably smaller CSA of the phosphorus compared to the protons directly involved in the hydrogen bonds. In a control experiment, the result of which is shown in Figure 3C, cross-peaks appear due to ^{31}P−^{1}H *J* couplings exclusively, qualitatively reproducing the correlations observed in Figure 3A. The sensitivity, however, was somewhat lower, because the underlying pulse sequence includes four additional 180°

(29) Brüschweiler, R. *Chem. Phys. Lett.* **1996**, *257*, 119−122.
(30) (a) Bendall, M. R.; Pegg, D. T.; Doddrell, D. M. *J. Magn. Reson.* **1983**, *52*, 81−117. (b) Bax, A.; Griffey, R. H.; Hawkins, B. L. *J. Magn. Reson.* **1983**, *55*, 301−315.
(31) Clore, G. M.; Murphy, E. C.; Gronenborn, A. M.; Bax, A. *J. Magn. Reson.* **1998**, *134*, 164−167.
(32) Bax, A.; Vuister, G. W.; Grzesiek, S.; Delaglio, F.; Wang, A. C.; Tschudin, R.; Zhu, G. *Methods Enzymol.* **1994**, *239*, 79−105.
(33) Vuister, G. W.; Bax, A. *J. Magn. Reson., B* **1993**, *102*, 228−231.
(34) (a) Löhr, F.; Pérez, C.; Schmidt, J. M.; Rüterjans, H. *Bull. Magn. Reson.* **1999**, *20*, 9−14. (b) Löhr, F.; Rüterjans, H. *J. Magn. Reson.* In press.

Table 1. Trans Hydrogen Bond $^{1}H-^{31}P$ Coupling Constants and Geometric Parameters in *Desulfovibrio vulgaris* Flavodoxin

donor group	^{2h}J (Hz)[a]	$R_{O\cdots O(P)}$ or $R_{N\cdots O(P)}$ (Å)[b]	∠O−H···O(P) or N−H···O(P) (deg)[b]	∠(O)H···O−P or (N)H···O−P (deg)[b]
S10 OH	0.63 ± 0.14	2.49	168	115
T11 NH	0.63 ± 0.18	2.55	164	117
T12 OH	1.66 ± 0.14	2.50	175	143
T12 NH	0.5[c]	2.77	134	100
N14 NH	0.5[c]	2.98	165	116
T15 OH	0.95 ± 0.09	2.79	143	115
T15 NH	1.50 ± 0.15	2.62	156	128
S58 OH	0.68 ± 0.15	2.55	170	110

[a] Averages and maximal deviations of five separate measurements. Values are not corrected for differential relaxation due to ^{1}H spin flips. [b] Distances and bond angles are taken from the flavodoxin X-ray structure of ref 2i. [c] Estimated values because of insufficient signal-to-noise.

pulses, whose imperfections distort signal intensities. Therefore, spectra of the type of Figure 3A were used to quantitatively determine $^{2h}J_{PH}$ as calculated from the expression $I_C/I_A = \tan^2(\pi J\Delta)$, where I_C and I_A are intensities of cross-peaks and axial peak, respectively. The resulting coupling constants obtained for flavodoxin are summarized in Table 1.

The J values reported in Table 1 are averages from five separate [^{31}P,^{1}H]-HMQC experiments, recorded with Δ periods of 30, 32 (2×), 33, and 35 ms, and represent apparent coupling constants. They are affected by differential relaxation as a consequence of rapid proton spin flips during Δ. Assuming a selective R_1 proton relaxation rate of 8 s^{-1} it can be calculated[35] that the true coupling constants are underestimated by 10−13%, depending on the exact length of Δ. However, no systematic variation of the apparent J values with Δ was observed for the relatively narrow range employed here. Some systematic error is also introduced by using peak heights instead of integrated signal intensities for the evaluation of coupling constants. The former can be measured more reliably, but nonidentical line widths of cross-peaks and axial peak, resulting from different transverse relaxation rates of $^{1}H-^{31}P$ multiple quantum and ^{31}P single quantum coherences during t_1 as well as passive proton−proton couplings, lead to a further underestimation by approximately 5−10%. Signal intensities of ribityl-C5′ and -C3′ bound protons translate into $^{3}J_{PH}$ and $^{5}J_{PH}$ coupling constants of 2.53 ± 0.20 and 0.98 ± 0.09 Hz, respectively, where the errors denote the largest deviations from the average values, as in Table 1. It should be noted that the $^{31}P-^{1}H_{5'}$ cross-peak arises from two degenerate protons so that the measured coupling represents the maximum for either of the two vicinal interactions. Such small coupling constants are in accordance with a gauche−gauche configuration[36] of the phosphoester bond, as was previously found for various flavodoxins.[20b,20c,25]

All hydrogen bonds detected for *D. vulgaris* flavodoxin in this study correspond to N···O(P) or O$^{\gamma}$···O(P) distances shorter than 3.0 Å in its crystal structure resolved at 1.7 Å resolution[2i] (compare Figure 1). Consistent with N···O(P) distances of at least 4 Å, there was no indication for putative hydrogen bonds of the phosphate with Ser10 NH[22a,23] or one of the Asn14 side chain amide protons[23] which had been inferred solely on the basis of their low-field ^{1}H chemical shifts. This again stresses the inherent advantage of scalar couplings over other NMR parameters, unambiguously identifying not only the hydrogen donating but also the acceptor group. Note, however, that it is in principle impossible to determine by NMR which of the four phosphate oxygens is the acceptor atom for a particular hydrogen bond. A clear correlation between hydrogen bond lengths and $^{2h}J_{PH}$ values as observed for $^{3h}J_{NC'}$ in proteins[37] and for $^{2h}J_{NN}$ and $^{1h}J_{NH}$ in DNA base pairs[11b] is not apparent from the sparse data available here. Possible reasons could be the variation in O−H···O(P) or N−H···O(P) tilt angles[38] and the limited precision of both X-ray coordinates and NMR coupling constants. Furthermore, the magnitude of the couplings may also depend on the unknown covalent H−O and H−N distances[11b,39] in the respective hydrogen bonds.

Quantitative Determination of $^{h}J_{NP}$. Previously, scalar couplings across hydrogen bonds have not only been observed for the protons themselves but also for the heavy atoms of donor/acceptor groups.[10−17] From the results reported above, the amide groups of Thr11, Thr12, Asn14, and Thr15 therefore appeared to be possible candidates for $^{3h}J_{NP}$ couplings in *D. vulgaris* flavodoxin. To examine the presence of such interactions a $^{1}H,^{15}N,^{31}P$-triple resonance experiment has been carried out on a ^{15}N-labeled flavodoxin sample. The pulse scheme is presented in the Supporting Information. It is a [^{15}N,^{1}H]-TROSY-type[40] $^{15}N-\{^{31}P\}$ spin−echo difference experiment that takes advantage of the partial cancellation of ^{15}N CSA and $^{1}H-^{15}N$ DD interactions during periods of ^{15}N transverse magnetization, allowing for relatively long $^{15}N-^{31}P$ de- and rephasing times Δ. As mentioned above in the context of the [^{1}H,^{31}P]-HMBC experiments, the discrimination of ^{31}P chemical shifts is unnecessary in the case of flavodoxin, such that the experiment could be carried out in a two-dimensional rather than a three-dimensional version resulting in $^{1}H-^{15}N$ correlation maps. The price to be paid for omitting a ^{31}P spectral dimension is that reference intensities needed for a quantification of $^{15}N-^{31}P$ couplings cannot be derived from axial peaks in the same spectrum in the manner of the [^{31}P,^{1}H]-HMQC method, and reference spectra had to be recorded separately.

A 2D $^{1}H,^{15}N-\{^{31}P\}$ spin−echo difference spectrum of flavodoxin is shown together with the corresponding reference spectrum in Figure 4, spectra A and B, respectively. One cross-peak, unambiguously assigned to Thr15 NH was detected with high signal-to-noise, whereas no indication of correlations corresponding to Thr12 or Asn14 was obtained. The experiment was performed twice with Δ = 75 ms and once with Δ = 90 ms. The $^{3h}J_{NP}$ coupling constant of the Thr15 amide determined from the ratio of cross/reference peaks intensities in the three pairs of experiments ranged between 1.71 and 1.77 Hz, indicating a high precision of this measurement. In two of the spectra very weak cross-peaks were observed at the $^{1}H-^{15}N$ resonance positions of Thr11, from which $^{3h}J_{NP}$ coupling constants of 0.28 (at Δ = 75 ms) and 0.25 Hz (at Δ = 90 ms), respectively, can be calculated. From the complete absence of Thr12 or Asn14 correlations, which exhibited lower reference peak intensities compared to Thr11, the upper limit of potential $^{3h}J_{NP}$ interactions of these amides is estimated to be 0.25 Hz.

Differential relaxation of ^{15}N in-phase and antiphase magnetization with respect to ^{31}P leads to an underestimation of

(35) (a) Vuister, G. W.; Bax, A. *J. Am. Chem. Soc.* **1993**, *115*, 7772−7777. (b) Kuboniwa, H.; Grzesiek, S.; Delaglio, F.; Bax, A. *J. Biomol. NMR* **1994**, *4*, 871−878. (c) Ponstingl, H.; Otting, G. *J. Biomol. NMR* **1998**, *12*, 319−324.

(36) (a) Cozzone, P. J.; Jardetzky, O. *Biochemistry* **1976**, *15*, 4860−4865. (b) Lankhorst, P. P.; Haasnoot, C. A. G.; Erkelens, C.; Altona, C. *J. Biomol. Struct. Dyn.* **1984**, *1*, 1387−1405.

(37) Cornilescu, G.; Ramirez, B. E.; Frank, M. K.; Clore, G. M.; Gronenborn, A. M.; Bax, A. *J. Am. Chem. Soc.* **1999**, *121*, 6275−6279.

(38) Scheurer, C.; Brüschweiler, R. *J. Am. Chem. Soc.* **1999**, *121*, 8661−8662.

(39) Benedict, H.; Shenderovich, I. G.; Malkina, O. L.; Malkin, V. G.; Denisov, G. S.; Golubev, N. S.; Limbach, H.-H. *J. Am. Chem. Soc.* **2000**, *122*, 1979−1988.

(40) Pervushin, K.; Riek, R.; Wider, G.; Wüthrich, K. *Proc. Natl. Acad. Sci. U.S.A.* **1997**, *94*, 12366−12371.

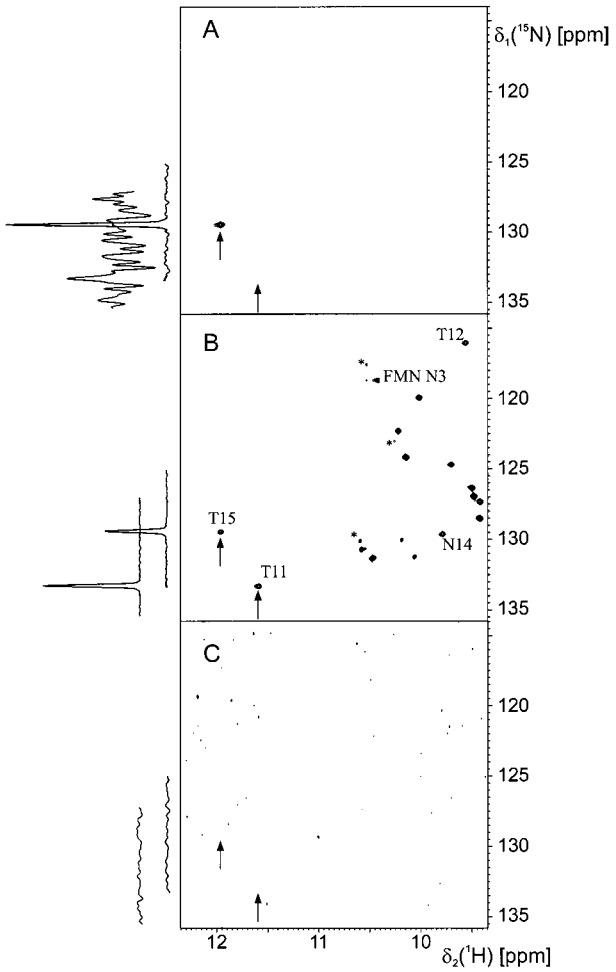

Figure 4. (A) ^{31}P-selected [^{15}N,^{1}H]-TROSY spectrum of flavodoxin recorded with the pulse sequence in Figure 1 of the Supporting Information using a Δ period of 75 ms. The only observable ^{15}N−^{31}P connectivities belong to the backbone amide groups of Thr15 and Thr11 (very weak). The cross-peak of Thr11 appears below the plotted level. The corresponding reference spectrum shown in part B is employed to calculate $^{3h}J_{NP}$ coupling constants. Assignments for cross-peaks of NH groups relevant for FMN binding are indicated. The FMN N3 signal is aliased along the F1 dimension and corresponds to a ^{15}N chemical shift of 159.7 ppm. Asterisks mark minor "anti-TROSY" components of very strong signals. The spectrum in part C, which is plotted near the noise level, was recorded with the same parameters as that of part A, but with a modified pulse sequence, exclusively allowing a polarization transfer via ^{15}N CSA/^{31}P−^{15}N DD relaxation interference. F1 traces on the left side of each contour plot, taken at the positions indicated by arrows, are identically scaled in A, B, and C, except for the Thr11 trace (at F2 = 11.6 ppm) in part A, which is expanded 10 times. Note that the spectrum of part B was acquired with 16 times fewer scans.

the true coupling constant in the order of 5−10% for an estimated phosphorus longitudinal relaxation rate around 1 s^{-1}. The presence of significant ^{15}N CSA/^{31}P−^{15}N DD cross correlation contributions could be ruled out using a modified version of the pulse sequence which selects for the latter interaction but suppresses scalar couplings. In the resulting spectrum, depicted in Figure 4C, no cross-peaks at all were detected with Δ = 75 ms.

As judged from the $^{2h}J_{HP}$ coupling constants of the four amide groups in the phosphate binding site in flavodoxin, the NH···OP hydrogen bond of Thr15 is considerably stronger than that of Thr11 and especially those involving Thr12 and Asn14. This picture is qualitatively confirmed by the $^{3h}J_{NP}$ measurements, although the much more pronounced difference between the values determined for Thr11 and Thr15 was unexpected and is not in accord with almost identical crystallographic N···O(P) distances and N−H···O(P) bond angles. One possible explanation might be the variation in (N)H···O−P angles (see Table 1), which should have an influence on the degree of overlap between electronic orbitals participating in the hydrogen bond and the O−P covalent bond, as was discussed recently in the context of relative magnitudes of $^{3h}J(^{15}N-^{13}CO)$ couplings in proteins and nucleic acids.[13] In this respect it is interesting to note that the largest $^{2h}J_{HP}$ coupling in flavodoxin was measured for the most linear arrangement of the participating atoms, i.e., Thr12 O−H···O−P.

The fact that $^{3h}J_{NP}$ interaction across the phosphate-Thr15 NH hydrogen bond is larger than $^{2h}J_{HP}$ (≈1.7 vs 1.5 Hz) despite the 10 times smaller gyromagnetic ratio and the larger distance strongly hints at a scalar rather than a dipolar nature of the couplings. Given the crystallographic distances in the phosphate binding site of flavodoxin, a dipolar contribution to $^{2h}J_{HP}$ or $^{3h}J_{NP}$ of 0.5 Hz would require a molecular alignment which gives rise to $^{1}D_{NH}$ splittings of at least 2 and 50 Hz, respectively, assuming identical orientations of the internuclear vectors with respect to the magnetic susceptibility tensor. Both values are beyond what is typically observed for diamagnetic proteins in the isotropic phase.[26b] Therefore, residual dipolar couplings as a source of the detected ^{1}H−^{31}P and ^{15}N−^{31}P interactions can be ruled out.

Conclusions

The presence of ^{1}H−^{31}P and ^{15}N−^{31}P scalar couplings observed in this study suggests a covalent character to the hydrogen bonds between the FMN phosphate and the apoprotein in *D. vulgaris* flavodoxin. As a consequence, the formally 2-fold negative charge on the phosphate would be partially delocalized on the adjacent backbone NH and side chain OH groups thus reducing its electrostatic contribution to the remarkably low redox potential of the flavin semiquinone/hydroquinone couple. This is in line with recent investigations on *D. vulgaris* flavodoxin mutants,[41] but contrasts with earlier theoretical calculations which suggested that the phosphate accounts for a significant portion of the unfavorable electrostatic interactions experienced by the N1 nitrogen of the FMN isoalloxazine portion in the hydroquinone state.[42] It seems likely that the considerably less negative redox potential determined in a complex between *D. vulgaris* apoflavodoxin and riboflavin,[43] which lacks the 5′-phosphate group, results to a large extent from the loss of hydrogen bonding contacts rather than from removal of the negative charges. From the crystal structure of this complex[2n] it was concluded that the FMN phosphate plays a role in the optimal positioning of the flavin to the protein and stabilizing the otherwise flexible ribityl chain of the cofactor.

To our knowledge, the measurements described here present the first data about trans hydrogen bond *J* couplings involving a phosphorus nucleus. These couplings are able to provide insight into strong cofactor−apoprotein interactions in flavodoxins and possibly in other flavoproteins. Furthermore, their existence may indicate a way to identify intermolecular hydrogen bonds in protein−nucleic acid complexes.

(41) (a) Zhou, Z.; Swenson, R. P. *Biochemistry* **1995**, *34*, 3193−3192. (b) Zhou, Z.; Swenson, R. P. *Biochemistry* **1996**, *35*, 12443−12454.

(42) Moonen, C. T. W.; Vervoort, J.; Müller, F. In *Flavins and Flavoproteins*; Bray, R. C., Engel, P. C., Mayhew, S. G., Eds.; Walter de Gruyter & Co.: Berlin, 1984; pp 493−496.

(43) (a) Curley, G. P.; Carr, M. C.; Mayhew, S. G.; Voordouw, G. *Eur. J. Biochem.* **1991**, *202*, 1091−1100. (b) Pueyo, J. J.; Curley, G. P.; Mayhew, S. G. *Biochem. J.* **1996**, *313*, 855−861.

Experimental Section

Recombinant *Desulfovibrio vulgaris* flavodoxin was expressed and purified according to previously reported protocols.[43a] For NMR experiments, the protein samples were dissolved to final concentrations of 7 mM (unlabeled) and 4 mM (^{15}N-labeled) in 0.5 mL of 10 mM potassium phosphate buffer, pH 7, containing 5% D_2O.

All NMR experiments were carried out on Bruker Avance spectrometers operating at ^{1}H frequencies of 800.13 or 499.87 MHz with the temperature adjusted to 305 K. Proton-detected [^{1}H,^{31}P]-HMBC and ^{15}N−{^{31}P} spin−echo difference experiments, performed at 800.13 MHz, employed a 5 mm ^{1}H/^{31}P/^{13}C/^{15}N quadruple resonance probe equipped with actively shielded three-axis pulsed-field gradient (PFG) coils. ^{31}P-detected [^{31}P,^{1}H]-HMQC spectra were recorded at 499.87 MHz proton resonance frequency using a 5 mm broadband observe probe without PFG accessory. Spectra were processed with the Bruker XWIN NMR 2.1 software.

The [^{1}H,^{31}P]-HMBC pulse sequence for recording the 1D spectrum shown in Figure 2A was $90°\phi_1(^1H)-\Delta-90°\phi_2(^{31}P)-G1-90°\phi_3(^{31}P)-G2-Aq(^1H)$. The ^{31}P carrier frequency was placed at the FMN phosphate resonance (4.96 ppm) and the 90° pulse width was adjusted to avoid excitation of the phosphate buffer signal. The proton carrier was centered at 8.0 ppm. Sine-bell shaped PFG's were applied with strengths of G1 = 40 G/cm and G2 = −23.8 G/cm (=G1 × (γP/γH − 1)) and durations of 0.8 ms. For optimal water suppression equal relative strengths along the *x*, *y*, and *z*-axes were employed to obtain magic-angle gradients.[44] Pulse phases were cycled according to $\phi_1 = 2(x), 2(-x)$, $\phi_2 = x, -x$, $\phi_3 = 4(x), 4(-x)$, $\phi_{rec} = x, 2(-x), x, -x, 2(x), -x$. A total of 114688 transients were accumulated, giving rise to a measurement time of 43 h. The versions of the pulse sequence for exclusive detection of ^{1}H CSA/^{1}H−^{31}P dipolar interactions (Figure 2B) and scalar couplings (Figure 2C) were $90°\phi_1(^1H)-\Delta/2\ -180°(^1H)-\Delta/2-90°\phi_2(^{31}P)-G1-90°\phi_3(^{31}P)-G2-Aq(^1H)$ and $90°\phi_1(^1H)-\Delta/2-180°(^1H,^{31}P)-\Delta/2-90°\phi_2(^{31}P)-G1-90°\phi_3(^{31}P)-G2-Aq(^1H)$, respectively. To eliminate possible imperfections of the 180° pulses they were surrounded by a pair of 1-ms gradient pulses applied along the *x*-axis with a strength of 5 G/cm. Each of the two spectra results from 49152 transients acquired within 21 h using otherwise identical parameters as above.

Quantitative 2D ^{31}P−^{1}H correlation spectra such as that shown in Figure 3A were obtained with the reverse HMQC pulse sequence $90°\phi_1(^{31}P)-\Delta-90°\phi_2(^1H)-t_1/2-180°\phi_3(^{31}P)-t_1/2-90°\phi_4(^1H)-\Delta-Aq(^{31}P), Dec(^1H)$. ^{31}P and ^{1}H carrier positions were 3.8 and 10.7 ppm, respectively. Pulses on both nuclei were applied with an RF field strength of 28.4 kHz. Proton decoupling during acquisition was accomplished by a 3.7 kHz DIPSI-2[45] modulation. Phase cycles were $\phi_1 = x, -x$, $\phi_2 = -x$, $\phi_3 = 2(x), 2(y), 2(-x), 2(-y)$, $\phi_4 = x$, $\phi_{rec} = x, 2(-x), x$ in the real part and $\phi_1 = x, -x$, $\phi_2 = -y$, $\phi_3 = 2(x), 2(y), 2(-x), 2(-y)$, $\phi_4 = 8(x), 8(-x)$, $\phi_{rec} = 2[x, 2(-x), x], 2[-x, 2(x), -x]$ in the imaginary part of each t_1 increment, such that ^{31}P magnetization that is not transferred to ^{1}H during Δ is maintained in the former and canceled in the latter. This gives rise to a signal at zero offset in the indirect dimension, which can be exploited as reference peak.[46] The intensity of cross-peaks appearing in the same spectrum is not affected by the phase cycling scheme. Spectral widths covered 16.13 and 11.97 ppm in the ^{1}H and ^{31}P dimensions, respectively. 140 × 512 complex points were recorded, corresponding to acquisition times of 17.4 (t_1) and 105.7 ms (t_2). Accumulation of 1024 scans per FID resulted in a measurement time of 7.4 days for each experiment. The effect of ^{31}P CSA/^{31}P−^{1}H DD relaxation interference was probed using the pulse sequence $90°\phi_1(^{31}P)-\Delta/2-180°(^{31}P)-\Delta/2-90°\phi_2(^1H)-t_1/2-180°\phi_3(^{31}P)-t_1/2-90°\phi_4(^1H)-\Delta/2-180°(^{31}P)-\Delta/2-Aq(^{31}P), Dec(^1H)$. The phase cycle was the same as above, but the two additional 180°(^{31}P) pulse phases were independently alternated between *x* and −*x* without change of the receiver reference phase. Restriction of the ^{31}P−^{1}H polarization transfer to scalar couplings was achieved with the pulse sequence $90°\phi_1(^{31}P)-\Delta/2-180°(^{31}P,^1H)-\Delta/2-90°\phi_2(^1H)-t_1/2-180°\phi_3(^{31}P)-t_1/2-90°\phi_4(^1H)-\Delta/2-180°(^{31}P,^1H)-\Delta/2-Aq(^{31}P), Dec(^1H)$. The resulting spectra, B and C in Figures 3, respectively, were recorded within 6 days each, using 832 scans per increment. Prior to multiplication with a squared-cosine weighting function, t_1 time domain data in all spectra were extended to 200 complex points by linear prediction, while 10 Hz line broadening was applied in the t_2 domain.

$^{3h}J_{NP}$ coupling constants in ^{15}N-labeled flavodoxin were determined by a [^{15}N,^{1}H]-TROSY ^{15}N−{^{31}P} spin−echo difference experiment. The pulse scheme and experimental details are provided in the Supporting Information. Spectra were recorded with acquisition times of 38.1 and 91.8 ms, collecting 128 × 1024 complex data points in the t_1 and t_2 dimensions, respectively. Spectral widths were 41.11 ppm in F1 (^{15}N) and 13.95 ppm in F2 (^{1}H). For ^{31}P-selected experiments, 128 scans were acquired for each FID while 8 scans were used for reference experiments, resulting in measurement times of 17 h and slightly more than 1 h, respectively. The spectra were identically processed, employing linear prediction to 220 points in t_1 and squared-cosine apodization in both dimensions.

Acknowledgment. We thank Dr. Rüdiger Weisemann and Bruker Analytik GMBH (Rheinstetten, Germany) for the loan of a 500 MHz broadband observe NMR probe. The help of Dr. Martin Knauf with the expression and labeling of the *D. vulgaris* flavodoxin is gratefully acknowledged. Dr. Martin A. Walsh is thanked for providing the X-ray coordinates resolved at 1.7 Å. This work was supported by a grant from the Deutsche Forschungsgemeinschaft (SFB 472, P10).

Note Added in Proof

M. Mishima, M. Hatanaka, S. Yokoyama, T. Ikegami, M. Wälchli, Y. Ito, and M. Shirakawa (*J. Am. Chem. Soc.* **2000**, *122*, 5883−5884) recently have determined $^{2h}J_{HP}$ and $^{3h}J_{NP}$ coupling constants in a protein-nucleotide complex using methods similar to those described in this paper.

Supporting Information Available: Pulse sequence and description of the method for the measurement of $^{3h}J_{NP}$ coupling constants in flavodoxin (PDF). This material is available free of charge via the Internet at http://pubs.acs.org.

JA001345K

(44) Mattiello, D. L.; Warren, W. S.; Mueller, L.; Farmer, B. T., II *J. Am. Chem. Soc.* **1996**, *118*, 3253−3261.

(45) Shaka, A. J.; Lee, C. J.; Pines, A. *J. Magn. Reson.* **1988**, *77*, 274−293.

(46) Zhu, G.; Bax, A. *J. Magn. Reson. Ser. A* **1993**, *104*, 353−357.